Lab on a Chip

Detection of leukemia markers using long-range surface plasmon waveguides functionalized with protein G

Journal:	*Lab on a Chip*
Manuscript ID:	LC-ART-08-2015-000940.R1
Article Type:	Paper
Date Submitted by the Author:	03-Sep-2015
Complete List of Authors:	Krupin, Oleksiy; University of Ottawa, Engineering Wang, Chen; Mount Sinai Hospital, Berini, Pierre; University of Ottawa, School of Information Technology and Engineering

Lab on a Chip

ARTICLE

Detection of leukemia markers using long-range surface plasmon waveguides functionalized with protein G

Received 00th January 20xx,
Accepted 00th January 20xx

DOI: 10.1039/x0xx00000x

www.rsc.org/

O. Krupin,[a] C. Wang[b] and P. Berini[c,d,e]

A novel optical biosensor based on long-range surface plasmon-polariton (LRSPP) waveguides is demonstrated for the detection of leukemia markers in patient serum using a functionalization strategy based on Protein G. The sensor consists of thin straight Au waveguides (5μm × 35 nm ×3.2mm) embedded in fluoropolymer CYTOP™ with a fluidic channel etched into the top cladding. B-cell leukemia is characterized by a high B-cell count and abnormal distribution of immunoglobulin G kappa (IgGκ) and lambda (IgGλ) light chains in serum. The detection of leukemic abnormalities in serum was performed based on determining IgGκ-to-IgGλ ratios (κ:λ). Three patient sera were tested: high kappa (HKS, κ:λ ~12.7:1), high lambda (HLS, λ:κ ~6.9:1) and normal (control) sera (NS, κ:λ ~1.7:1). Au waveguides were functionalized with Protein G and two complementary immobilization approaches were investigated: a) the reverse approach, where the Protein G surface is functionalized with patient serum and then tested against goat anti-human IgG light chains in buffer, and b) the direct approach, where the Protein G surface is functionalized with goat anti-human IgGs first and then tested against patient serum. The reverse approach was found to be more effective and robust because Protein G-functionalized surface performs as an "immunological filter" by capturing primarily IgGs out of the pool of serum proteins. For the reverse approach, the ratios measured were 3.7:1(κ:λ), 9.7:1(λ:κ) and 1.9:1(κ:λ) for HKS, HLS and NS, respectively, which compare favorably with corresponding protein densitometry measurements. The respective ratios for the direct approach were 2.6:1(κ:λ), 2.6:1(λ:κ) and 1.7:1(κ:λ). The binding strength and cross-reactivity of goat anti-human IgGs light chains were also determined using pure solutions. The LRSPP biosensor along with the innovative "reverse approach" can provide a low-cost and compact solution to B-cell leukemia screening.

Introduction

B-cell tumors such as Waldenström's disease, plasma cell neoplasms, chronic lymphocytic leukemia (CLL) and lymphomas, are often associated with monoclonal immunoglobulin production. Currently, there is no standard procedure for early leukemia detection,[1] and most of the diagnostic tests include complex procedures such as blood cell morphology, bone marrow biopsy or flow cytometry. While the normal immunoglobulin G (IgG) kappa-lambda light chain ratio in serum ranges from 1.4-2:1[2], due to overproduction of monoclonal IgGs in B-cell tumors, either lambda or kappa immunoglobulins can dominate. Recent studies in this area suggested the possibility of detecting B-cell tumors based on the proportion of immunoglobulin kappa (IgGκ) and lambda (IgGλ) light chains in serum.[2-4] In addition, it has been shown that patients with an abnormal light chain ratio are prone to more aggressive disease progression and require early treatment.[5] Traditional tests for the IgGκ:IgGλ ratio are serum or urine protein electrophoresis (SPE, UPE) and turbidimetric methods such as densitometry. Although these methods may be satisfactory, there are existing problems. One example is the case where immunoglobulin bands overlie other proteins (such as transferrin) and are detectable only by immunofixation electrophoresis (IFE), which is nonquantitative.[6] Thus, new methods of immunoglobulin light chain detection in serum are of interest.

Optical biosensors have become appealing in the past 20 years due to their ability to quickly detect biomolecules in real-time without prior labeling. Other additional benefits such as the small consumption of analytical ingredients and no requirements for well-trained personnel make optical biosensors competitive to common clinical diagnostic techniques such as ELISA, flow cytometry or bacterial culture. Still, the main current application of optical

[a] Department of Biological and Chemical Engineering, University of Ottawa, 161 Louis Pasteur, Ottawa, Ontario, K1N 6N5, Canada.
[b] Department of Pathology and Laboratory Medicine, Mount Sinai Hospital, University of Toronto, 600University Ave., Toronto, M5G1X5, Canada.
[c] School of Electrical Engineering and Computer Science, University of Ottawa, 800 King Edward Ave., Ottawa, K1N6N5, Canada.
[d] Department of Physics, University of Ottawa, 150 Louis Pasteur, Ottawa, K1N 6N5, Canada.
[e] Centre for Research in Photonics, University of Ottawa, Ottawa, K1N 6N5, Canada.
† Footnotes relating to the title and/or authors should appear here.
Electronic Supplementary Information (ESI) available: [details of any supplementary information available should be included here]. See DOI: 10.1039/x0xx00000x

biosensors remains in the pharmaceutical field, where kinetics extraction of biomolecular interactions is the main interest.[7] The field of optical biosensors is currently dominated by the methods of surface plasmon resonance (SPR), which utilizes the Kretschmann-Raether configuration.[8,9]

Long-range surface plasmon-polaritons (LRSPPs) are surface plasmon waves that can propagate over appreciable lengths along a thin metal slab or stripe, bounded by dielectrics of similar refractive index (RI), upon optical excitation.[10] The LRSPP propagation length can extend to centimetres, whereas that of single-interface SPR is ~80 μm, so the former provides a longer interaction length with the sample to be measured leading to high-sensitivity.[11] The LRSPP field penetration depth is ~1 μm, and is significantly larger than that of SPR (~200 nm), which provides advantages when sensing large objects such as cells. Furthermore, a thicker layer of hydrogel dextran matrix can be deposited on the waveguide to capture more analyte thus further increasing the sensitivity of an LRSPP sensor.

LRSPP wave propagation along a metal stripe requires that the top and bottom dielectrics serving as claddings have similar refractive indices. Since most biological solutions are aqueous and have a low RI (~1.32), low-RI polymers such as CYTOP (Asahi) and Teflon (Dupont) have been utilized as a bottom cladding to maintain optical symmetry.[12-14]

LRSPPs have been investigated for biosensing by modifying an SPR prism-based sensor with Teflon, demonstrating increased sensitivity for bulk RI sensing,[12] showing a 5.5-fold increase in sensitivity for *E.coli* detection,[15] and in studying the effect of toxins on HEK-293 cells.[16] Due to wave confinement in the plane transverse to the direction of propagation, various waveguide configurations such as Y-junctions, S-bends and Mach-Zehnder Interferometers (MZIs) can be constructed.[17,18] Au MZIs with one etched arm have been successfully demonstrated for bulk sensing.[19]

The LRSPP biosensor described in this paper consists of a straight Au waveguide (SWG) embedded in CYTOP with a fluidic channel etched into the top cladding to expose the top surface of the Au stripe.[20] The LRSPP wave can be excited by butt-coupling an optical fibre to the waveguide input allowing the sensor to be potentially miniaturized. Our LRSPP sensor has been previously demonstrated for the detection of RI changes in bulk solutions and non-specific bovine serum albumin (BSA) adsorption.[21] Immunological detection of human red blood cells based on the ABO group demonstrated a limit of detection (LOD) one order of magnitude lower than SPR.[22] Dengue infection detection in patient plasma showed similar and better results compared to ELISA.[23] We also demonstrated the detection of gram-negative and gram-positive bacteria in urine.[24] In addition, the sensitivity[25] and optimization[26] of SWG LRSPP sensors has been investigated.

Non-metallic waveguides have also been used for biosensing applications.[27-29] However Au is a preferred surface for biosensing because it is chemically stable, it is the most studied, and it can be easily functionalized with sensing chemistries, especially thiol-based.[30]

Protein G is a streptococcal protein that has a strong affinity to the crystallizable fragment (Fc) of IgG and is commonly used for the purification of immunoglobulins. This property of Protein G becomes even more valuable for planar biosensors where the reacting immunoglobulins orient themselves “upward" thus exposing the fragment antigen-binding site (Fab) to the flowing solution carrying analyte. The application of Protein G for Au surface functionalization with IgG has been well-studied in SPR sensors. Different strategies have been explored for Protein G attachment to Au surface such as covalent attachment to alkanethiol self-assembled monolayer (SAM).[31] However, the simple adsorption of Protein G on Au at room temperature through Au-N interactions has also been shown to be successful for IgG functionalization,[32] and the kinetics of this interaction has been studied using SPR.[33]

The purpose of this study is to demonstrate the ability of LRSPP waveguide sensors to detect abnormalities in immunoglobulin kappa-lambda ratios in leukemic patient sera. Protein G surface functionalization was used for capturing IgGs. Experiments with pure analytes were performed as a proof-of-concept followed by testing of patient sera. Two different testing approaches were taken: the direct approach, where goat anti-human IgGs were injected on the Protein G surface, followed by the injection of patient serum, and the reverse approach, where the patient serum was injected over Protein G surface, followed by the injection of goat anti-human IgGs. We used the reverse approach to perform three repeats for each test. We prefer the reverse approach because it was found to have significant advantages such as: a) Protein G captures primarily IgGs out of the large variety of serum proteins, and b) the last sensing step involves flowing goat anti-human IgGs in clear buffer, which reduces (or completely eliminates) non-specific binding.

LRSPP waveguide biosensors define a new paradigm for the field - they are very sensitive and compact integrated optical structures, leveraging the attractive features of a Au sensing surface. An investigation of such sensors for detecting a relative ratio of similar proteins (immunoglobulins kappa and lambda) in a complex fluid (serum) is of interest. In addition, to our knowledge, only one study has investigated the detection B-cell leukemia based on measuring the κ-λ ratio with a biosensor (SPR).[34] Although strategies based on Protein G-functionalization are known, no attempt has been made to use the Protein G surface to "filter out" immunoglobulins from sera using biosensors. The reverse approach reported in this work suggests this strategy to be beneficial and promising for a variety of detection problems that involve immunoglobulins in complex fluids, irrespective of the biosensor type.

Experimental

Bio(chemicals)

2-Isopropanol (733458), acetone (270725), glycerol (49767), lyophilized bovine serum albumin (A0281), heptane (34873), sodium dodecyl sulfate (71725) and phosphate buffered saline (PBS, P5368) 0.01M, pH 7.4 were obtained from Sigma-Aldrich. PBS solution was prepared by dissolving packaged salts in 1L of distilled/deionized ($DDIH_2O$) water. Distilled water was deionized using Millipore filtering membranes (Millipore, Milli-Q water system at 16 MΩ•cm). Purified human IgG/kappa (P80-111) and purified human IgG/lambda (P80-112) were purchased from Bethyl Laboratories. Both samples contained all the isotypes of IgG. Goat anti-human kappa (GWB-8C381A) and goat anti-human lambda (GWB-298B63) were purchased from GenWay.

Patient samples

Three serum samples were used, collected from two patients with monoclonal immunoglobulin and a normal control. The sera were previously tested at the clinical laboratory of Mount Sinai Hospital, Toronto, Canada: 1) serum with highly abnormal concentration of IgG-kappa (HKS, total [IgG] = 21.6 g/L, monoclonal [IgG-kappa] = 17.4 g/L); 2) serum with highly abnormal

concentration of IgG-lambda (HLS, total [IgG] = 75.2 g/L, monoclonal [IgG-lambda] = 60 g/L); and 3) serum with normal ratio of IgG-kappa and IgG-lambda (NS, total [IgG] = 17.0 g/L). The data was obtained by protein densitometry - the standard clinical laboratory method that combines serum protein electrophoresis (SPE) for quantification of monoclonal protein and immunofixation electrophoresis (IFE) for identification of κ or λ chains of monoclonal immunoglobulins. The calculated κ-λ ratios for the three samples are presented in Table 1. The average values for the ratios arise from the variations in the distribution of the polyclonal IgGκ and IgGλ, which ranges from 1.4 to 2.0. The use of patient's samples was approved by Institutional Research Ethics Board.

Table 1. Monoclonal and polyclonal immunoglobulins in leukemic and normal patient samples.

Patient Sample	Polyclonal IgG, g/ml	Monoclonal IgG, g/ml	Average ratio	Estimated Error
High Kappa Serum (HKS)	4.2	17.4	12.7:1 (κ:λ)	±1.5
High Lambda Serum (HLS)	15.2	60.0	6.9:1 (λ:κ)	±0.5
Normal Serum (NS)	17.0	0	1.7:1 (κ:λ)	±0.3

Sensor description

A wafer, consisting of ~300 sensors was lithographically fabricated,[35,20] diced, and individual dies were used to perform the experiments. The sensing chip (3.2 mm × 6.4 mm) is comprised of Au waveguides (5 µm wide, 35 nm thick) embedded in CYTOP (Fig. 1). Fluidic channels were fabricated by etching the top CYTOP cladding down to the top Au surface. The plexiglas fluidic jig included a fluorocarbon O-ring (Apple Rubber Products Inc.) to provide a soft seal around the channel and two through holes inside the O-ring area for fluidic access. The whole assembly was fixed by two screws to a metal base. More details on the general sensing approach, the sensor, and our optical interrogation setup can be found in[21,22].

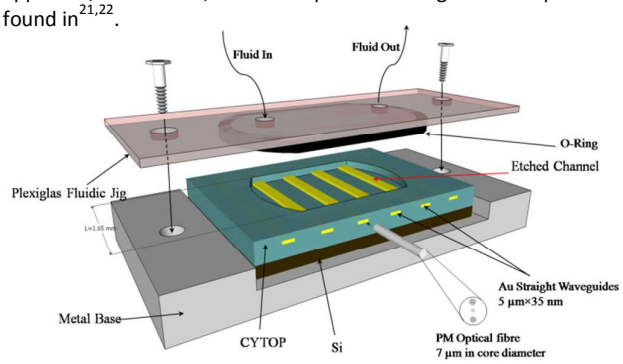

Fig. 1 Schematic representation of the sensor on the metal base with fluidic jig; the volume of the fluidic cell is 20 µL (Adapted from[22]).

Sensor preparation

Initially the whole wafer was covered with photoresist SPR-220 for surface protection during wafer dicing. Fiber-to-waveguide coupling is a delicate procedure, during which any mild contamination on the facet of the sensor can produce significant instability of the output signal. The facets were cleaned in an ultrasonic bath (Fisherbrand FB11201) in heptane for 5 minutes at 37 Hz (50% power). SPR-220 is resistant to heptane, thus keeping the etched surface protected from physical damage during ultrasonic cleaning. SPR-220 was removed by two acetone baths, the first for 5 min, and the second for 30 min, followed by an extensive IPA wash, and drying with N_2. Finally, the sensor was placed into a UV/Ozone chamber (Novascan, PSD-UV4) for 15 min with the UV lamp on and 15 min with the UV lamp off to remove any possible organic contaminants.

Surface functionalization and sensing protocols

As a sensing buffer, a mixture of PBS and glycerol (PBS/Gly) having a RI of n=1.338 was used throughout all experiments.[26] After full integration with fluidics and optics, the Au waveguides were functionalized with Protein G by injecting 50 µg/ml of protein in PBS/Gly for 25 min at a flowrate of 20 µl/min into the fluidic cell.

After Protein G functionalization, one of two different sensing strategies was applied as schematically presented in Fig. 2. The reverse approach (Fig. 2a) first involved the injection of patient serum (1:150 dilution with PBS/Gly) for capturing immunoglobulins out of the sample followed by the injection of goat anti-human light chain IgGs (either anti-kappa or anti-lambda). Patient serum was injected for 40 min at a 10 µl/min flowrate to ensure full surface coverage, and goat anti-human light chain IgGs (50 µg/ml) was flowed for 20 min at 10 µl/min. The direct approach (Fig. 2b), on the contrary, first involved functionalization of the protein G layer with goat anti-human light chain IgGs (50 µg/ml, 40 min at 10 µl/min) and the subsequent introduction of the patient serum. In the direct approach, the three patient sera had different dilutions to produce a concentration of the prevailing IgG light chain type (kappa or lambda) to 5 µg/ml. Details on the rationale of choosing dilution factors are provided later in this Section.

After each experimental stage, the surface was washed with PBS/Gly for ~10 min at a 20 µl/min flowrate to remove unbound analyte and re-establish the baseline. Regeneration of the surface down to the Au level after an experiment was performed by flushing the fluidic cell with SDS (0.5% w/w) for 20 min, then DDI H_2O for 20 min, then the sensor was removed from the fluidic cell, washed with plenty of IPA, dried with N_2 and placed into a UV/Ozone chamber with 15 min lamp on and 15 min lamp off.

During fabrication, small imperfections might result in waveguides not being identical. To eliminate potential inconsistencies in response, the same waveguide was used to test a single patient serum using surface regeneration and full re-functionalization for both approaches. Preliminary experiments and overall analysis suggest the reverse approach to be more sensitive and more robust than the direct approach (See the Results and Discussion section). We thus exploited primarily the reverse approach by carrying out three repeats for each experiment. Single measurements were taken for the direct approach. A single batch for each IgG purchased was used throughout all experiments to maintain consistency.

Preliminary experiments for the direct strategy also incorporated a step consisting of the injection of BSA (1 mg/ml in PBS/Gly) to block non-specific binding sites. Blocking was tested after Protein G functionalization or after IgG functionalization (with no prior blocking). BSA injections did not produce any signal changes, indicating the surface was fully functionalized with Protein G or IgGs; the blocking step was therefore eventually abandoned to reduce the overall time of the experimental procedure. The results of BSA blocking are presented in the supplemental material (Fig. S1).

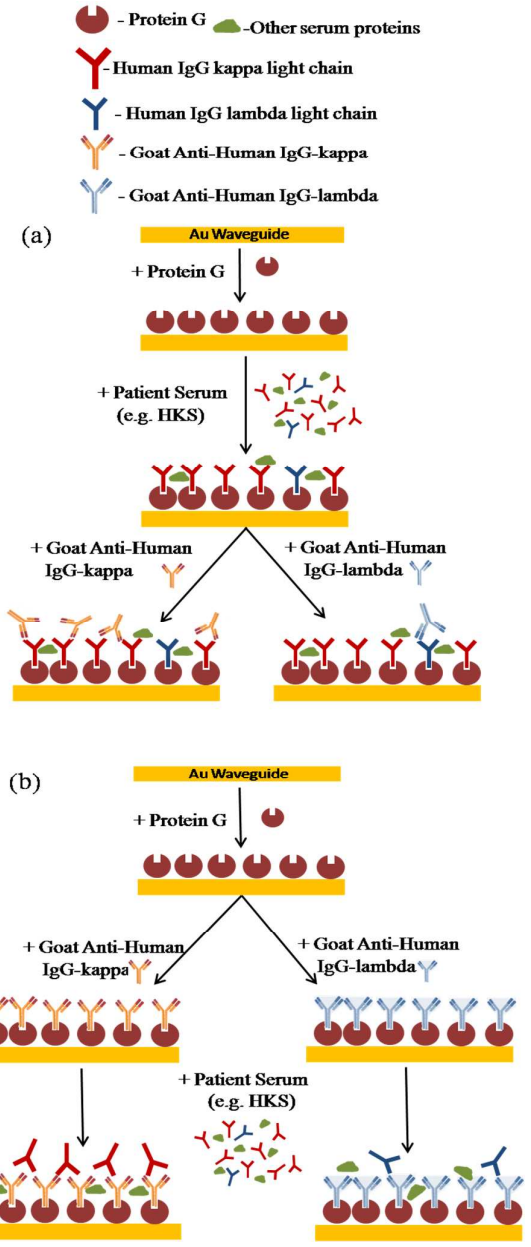

Fig. 2 Schematic illustration of two approaches for patient sample testing. (a) Reverse approach: The Au waveguide is functionalized with Protein G, followed by the immobilization of patient serum (example with HKS is shown), and finally, sensing with recognition goat anti-human kappa light chain IgG. The same waveguide is cleaned down to the Au level, and the whole experiment is repeated but the patient-functionalized surface is tested against goat anti-human lambda IgG. (b) Direct approach: The Au waveguide is functionalized with Protein G, followed by the immobilization of goat anti-human kappa IgG, and finally, sensing of patient serum (*e.g.* HKS). The same waveguide is cleaned down to Au level, and the experiment is repeated but with goat anti-human lambda IgG on the Protein G surface.

Rationale for dilution factors and concentrations

Concentrations of analyte for functionalization of Protein G layer

The kinetics of the Protein G-IgG interaction was studied using SPR, by adsorbing 50 µg/ml of Protein G on a Au surface, then injecting different concentrations of IgG.[33] Their study demonstrated that the Protein G surface was saturated with IgG molecules within 10 min, and the concentration sensitive region was below 667 nM (100 µg/ml). However, the concentration of 337 nM (50 µg/ml) produced a slightly (~3%) lower saturation level. Since in our study the final experimental step is to also capture IgGs, it is highly desirable to maintain the concentration of total IgG in the first injection step to above 50 µg/ml to completely saturate the Protein G surface. Otherwise, the IgGs to be detected in the final step will bind to Protein G instead, thus producing misleading results.

In the direct approach, in order to conserve the antibodies and consequently be able to use the same batches throughout all the experiments, a concentration of 50 µg/ml of goat anti-kappa and goat anti-lambda IgG was used to functionalize the Protein G surface.

The total IgG concentration in an adult is ~10 mg/ml.[36] For the reverse approach, all three patient sera were diluted to the dilution factor of 1:150 (serum:PBS/Gly). Thus, a 1:150 dilution of the average adult serum will result in at least ~67 µg/ml of total IgG, which is above the minimum desired value of 50 µg/ml. The 1:150 dilution of the three patient sera resulted in the following total IgG concentrations: NS = 113.3 µg/ml, HKS = 144.0 µg/ml and HLS = 501.3 µg/ml.

Concentrations of analyte used for functionalization and detection

For the direct approach, the last step is the introduction of patient serum. Preliminary experiments suggested that the concentration sensitive region ranges from 1 µg/ml to 10 µg/ml for pure human IgG-κ and IgG-λ, which is similar to the range previously measured by SPR.[34] Thus, for experiments with standard immunoglobulins, 5 µg/ml of either human IgG-κ or IgG-λ were used. For testing patient serum, all three sera were diluted to have a concentration of the dominant IgG light chain of 5 µg/ml: NS = 1:3400 dilution (~5 µg/ml of IgG-κ and ~2.9 µg/ml of IgG-λ), HKS = 1:4000 dilution (~5 µg/ml of IgG-κ and ~0.4 µg/ml of IgG-λ) and HLS = 1:15000 dilution (~5 µg/ml of IgG-λ and ~0.7 µg/ml of IgG-κ).

Preliminary results demonstrated that the concentration-dependent region for the interaction of human IgG and goat anti-human IgG ranged from 5 µg/ml to 30 µg/ml of goat anti-human IgG. In order to ensure full surface saturation for the direct approach, a concentration of 50 µg/ml of the goat anti-kappa and anti-lambda IgGs was used.

Due to the complexity of the experiments, a color scheme was applied to assist in the description of the results. It is presented in Table 2, along with the abbreviations. Generally, all solutions associated with a high content of kappa light chain are colored red and the ones associated with a high content of lambda light chain are blue. Goat anti-human kappa and anti-human lambda are also often referred to as recognition IgGs.

Table 2. Abbreviations and color schemes used throughout the paper.

Sample	Abbreviation
High Kappa Serum	HKS
High Lambda Serum	HLS
Normal Serum	NS
Goat anti-human kappa IgG light chain	AK
Goat anti-human lambda IgG light chain	AL
Human IgG-kappa	IgGκ
Human IgG-lambda	IgGλ
Protein G	PG

Results and discussion

Validation with pure analyte

Tests with standard analytes in clean solutions were performed to verify the specificity and cross-reactivity of recognition IgGs (AK and AL). The full experiments are presented in the supplemental material (Fig. S2), and summarized in what follows.

Fig. 3 presents the experimental responses for both approaches including cross-reactivity. For the reverse approach, IgGκ- (Fig. 3a) and IgGλ-functionalized (Fig. 3b) surfaces were tested by injecting either AK or AL for 20 min. The responses in both cases are as expected: high signal change for the matching immunoglobulin pairs (IgGκ-AK and IgGλ-AL) and low signal change for the opposite pairs (IgGκ-AL and IgGλ-AK). The same effect is observed for the direct approach (Fig. 3c and Fig. 3d), where the human IgGs were injected over AK- and AL-functionalized surfaces. For the complementary immunoglobulins a clear binding curve is observed confirming a specific and strong interaction. Very little change in baseline is observed for the opposite immunoglobulins suggesting a weak reaction due to cross-reactivity.

Purchased IgGs (both human and anti-human) already contained a buffer that had a significantly different RI than the sensing buffer (n=1.338). Upon dilution with PBS/Gly of AK and AL down to 50 µg/ml, the overall refractive index remained far from 1.338, producing a bulk step in the responses as seen in Fig. 3a and Fig. 3b. However, for the direct approach, the bulk step is much less significant because the initial solution of immunoglobulins was diluted down to 5 µg/ml. Small bulk steps that can be observed at the beginning and the end of each experiment are due to the stop/start of the flow. CYTOP is a mildly compressible polymer, and when the pressure in the system changes, the top cladding either becomes compressed or decompressed slightly changing the overall refractive index of the top cladding.

The results for both approaches are summarized in Fig. 4. The details of the binding strength calculations are presented in the patient testing section and the computed data are presented in supplemental material (Table S3A and S3B). For the reverse approach, the ratio of the complementary response to the cross-reactivity is 15.2 and 9.0 for kappa and lambda surfaces respectively. For the direct approach the ratios are 6.4 and 3.3, which are significantly lower and likely attributed to the limitations of the direct approach when concentrations of the tested analyte (human IgGs) have to be in the concentration-sensitive region, thus the overall response of the matching IgGs is lowered. In addition, the binding strength for kappa-anti-kappa and lambda-anti-lambda interactions is also significantly stronger using the reverse approach compared to the direct approach (~60 g/g *vs*. ~20 g/g).

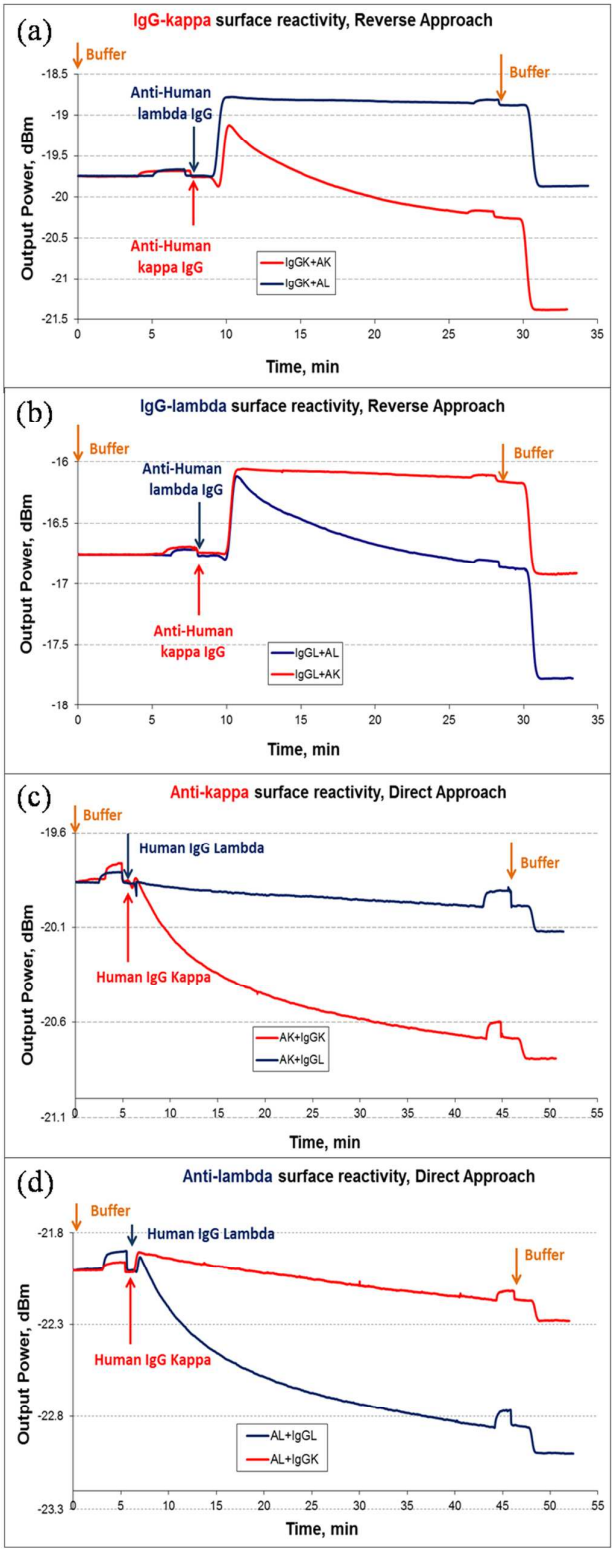

Fig. 3. Real time interaction of human IgG kappa/lambda and goat anti-human kappa/lambda for both approaches. Reverse approach: (a) Reactivity of IgGκ-functionalized surface for AK and AL. (b) Reactivity of IgGλ-functionalized surface for AK and AL. Direct approach: (c) Reactivity of AK-functionalized surface for IgGκ and IgGλ, (d) Reactivity of AL-functionalized surface for IgGκ and IgGλ.

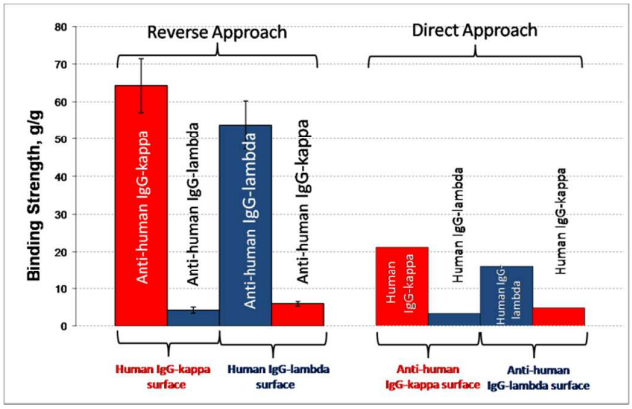

Fig. 4. Validation and comparison of both approaches using standard human IgGκ and IgGλ. The binding strength here is a measure of the mass of the recognition IgG bound, per mass of IgG reacted to Protein G [g/g].

Patient sample testing

Examples of full experiments for both approaches are presented in Fig. 5. For the reverse approach three repeated runs for determining the response of the HKS sample to AK are shown in Fig. 5a. Slight power level adjustments were performed at the initial baseline to align the responses (t=0, power output ~0.5 dBm), and the timescale for run 2 was adjusted to fit those of the other two runs. Although all three experiments were performed using three different sensors, the repeatability is very satisfactory showing only slight deviations in power output at the end of the experimental runs. One full experimental run for the direct approach, also for the HKS-AK test, is shown in Fig. 5b. In all cases the response for Protein G is significantly lower than for the next immunoglobulin functionalization step (~0.5 dB *vs.* ~ 2 dB). This is in agreement with the fact that Protein G is a smaller protein with a MW of ~65 kDa compared to IgG (~150 kDa), and since the attenuation of the LRSPP wave on the waveguide is proportional to the adsorbed mass,[26] larger molecules should produce stronger responses.

Visually the main difference between the two approaches is the bulk RI mismatch of the goat anti-human IgG solution, which creates a bulk step at the solution injection point and after the PBS/Gly wash (~100-120 min in the reverse, and ~45-95 min in the direct approaches respectively). It is hard to visually compare the responses of the final binding curves (anti-kappa in reverse and HKS in direct approaches) because of the bulk step in the reverse approach. The fluid exchange time in the system is ~2 min,[21] therefore, during this time period both binding and fluid exchange occur simultaneously, and if there is an RI mismatch between the sensing solution and the sensing buffer, the first two minutes do not represent the actual binding event. In this case, the anti-human kappa IgG solution has a lower RI than the PBS/Gly pulling the overall optical symmetry closer to the CYTOP RI, thus increasing the output power. On the other hand, binding of the IgGs to the surface increases the attenuation lowering the output power. The actual responses for all the three patient samples using both approaches are presented in the supplemental material (Fig. S4).

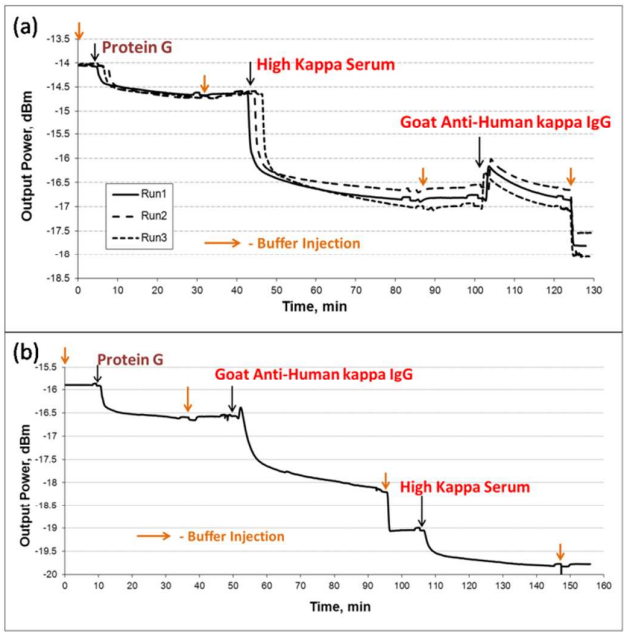

Fig. 5. Full experimental runs for testing HKS using both approaches: (a) Reverse approach showing three repeats; (b) Direct approach.

Slight variations in the quality of an individual sensor over the wafer are possible due to uneven gold evaporation, CYTOP distribution on the surface, and other fabrication imperfections. These variations can potentially create differences in the response such as seen in Fig. 5a. Since the purpose of the study is to compare the ratio of the amounts of two different analytes in the same solution, these slight variations can produce misleading results. In order to minimize the effect of variable sensor quality, a response was normalized to the response of the first immunoglobulin functionalization step (goat anti-human IgGs for direct or human IgGs for reverse approaches).

A mathematical expression relating the surface mass density to the power change due to adlayer formation on a straight waveguide is:[26,37]

$$\Delta\Gamma = \frac{1}{k_2}\frac{(n_a - n_c)}{\delta n/\delta c}\left(\frac{P_{out}(a_1)}{P_{out}(a_0)} - 1\right)$$

where $\Delta\Gamma$ is a change in surface mass density, k_2 is a constant that is specific for an individual sensor and is a function of variations in fabrication, n_a and n_c are the refractive indices of the adlayer material and the sensing fluid respectively, $\delta n/\delta c$ is a partial change of refractive index relative to a change in concentration of the adlayer matter in fluid. For proteins n_a ~1.5 and $\delta n/\delta c$ is relatively constant and equal to 0.185 mm^3/mg,[38] $P_{out}(a_0)$ and $P_{out}(a_1)$ are the output powers (in watts) before and after adlayer formation respectively.

Normalization of the response was performed by taking a ratio of $\Delta\Gamma$ of the second IgG step to $\Delta\Gamma$ of the first IgG step:

$$\frac{\Delta\Gamma(analyte)}{\Delta\Gamma(surface)} = \frac{\left(\frac{P_{out}(a_1)}{P_{out}(a_0)} - 1\right)_{analyte}}{\left(\frac{P_{out}(a_1)}{P_{out}(a_0)} - 1\right)_{surface}}$$

The term $\frac{1}{k_2}\frac{(n_a - n_c)}{\delta n/\delta c}$ cancels out because these parameters remain constant during a single experiment. From the biochemical point of view the ratio $\Gamma(\text{analyte})/\Gamma(\text{surface})$, if taken as a function of time, describes the rate of analyte binding to the surface and can be taken as the binding strength. Thus, $\Delta\Gamma(\text{analyte})/\Delta\Gamma(\text{surface})$ is an overall binding strength and is entirely related to the responses produced on the waveguide regardless of the sensor quality. Finally, in order to estimate the κ-λ ratio in a patient sample, the ratio of the binging strengths for kappa and lambda was computed. The detailed results of the aforementioned computations for HKS, HLS and NS are presented in Table 3. Computed data for all three sera for the direct approach is presented in supplemental material (Table S5).

Replicates for the reverse approach also demonstrate the quality of the experimental repeatability. For the HKS sample the $[P_{out}(a_1)/P_{out}(a_0) - 1] \times 100$ term for the HKS response on the Protein G surface varies from ~50 to ~60, which represents a ~18% difference. However, when taking the ratio of $\Delta\Gamma(analyte)/\Delta\Gamma(HKS)$ for each experimental run, the percentage difference is reduced to ~6% supporting the validity of the "binding strength approach" to analyze the data. For normal and high kappa serum the ratios of κ:λ were calculated, whereas for high lambda serum it was the reverse ratio (λ:κ).

Table 3. Experimental results and computational analysis to obtain κ-λ ratio for HKS, HLS and NS; reverse approach.

Patient Sample	Replicate	Step	Response $\left[\frac{P_{ao}}{P_{a1}} - 1\right] \times 100$	Binding Strength, g/g $\left[\frac{\Delta\Gamma(\text{recognitionIgG})}{\Delta\Gamma(\text{serum response})}\right] \times 100$	IgG light chain Ratio
High Kappa Serum	1	PG+HKS	59.96	47.09	3.17 (κ:λ)
		HKS +AK	28.23		
		PG+HKS	58.12	14.87	
		HKS+AL	8.64		
	2	PG+HKS	52.41	49.96	3.37 (κ:λ)
		HKS +AK	26.18		
		PG+HKS	49.97	14.81	
		HKS+AL	7.40		
	3	PG+HKS	51.71	48.16	3.38 (κ:λ)
		HKS +AK	23.88		
		PG+HKS	54.17	13.66	
		HKS+AL	7.40		
Average Ratio					**3.31 (κ:λ)**
Standard Deviation					**0.12**
High Lambda Serum	1	PG+HLS	65.20	38.83	11.32 (λ:κ)
		HLS+AL	25.31		
		PG+HLS	61.06	3.43	
		HLS+AK	2.09		
	2	PG+HLS	64.44	33.55	8.08 (λ:κ)
		HLS+AL	21.62		
		PG+HLS	61.81	4.15	
		HLS+AK	2.57		
	3	PG+HLS	60.32	40.06	9.83 (λ:κ)
		HLS+AL	24.17		
		PG+HLS	62.93	4.08	
		HLS+AK	2.57		
Average Ratio					**9.74 (λ:κ)**
Standard Deviation					**1.62**
Normal Serum	1	PG+NS	64.44	41.54	1.87(κ:λ)
		NS +AK	26.77		
		PG+NS	71.40	22.24	
		NS+AL	15.88		
	2	PG+ NS	65.96	42.36	1.72(κ:λ)
		NS +AK	27,94		
		PG+NS	61.06	24.70	
		NS+AL	15.08		
	3	PG+ NS	58.12	44.55	1.84(κ:λ)
		NS +AK	25.89		
		PG+NS	67.88	24.18	
		NS+AL	16.41		
Average Ratio					**1.81(κ:λ)**
Standard Deviation					**0.08**

The final results for patient testing are summarized in Fig. 6 (extracted from Tables 3 and S5) and compared to the data provided by the Mount Sinai Hospital laboratory (Table 1). The yellow stripe indicates the region of normal light chain immunoglobulin ratios: 1.4-2:1 for κ:λ and 0.5-0.7:1 for λ:κ. Overall, both approaches demonstrated the ability to detect abnormality in the IgGκ-IgGλ ratio in patient sera, as well as producing a normal ratio for the control (normal) patient serum.

For HKS, the three experimental repeats of the reverse approach show similar results with the average κ:λ being 3.3:1 and a low standard deviation of 0.12. However, these results are lower than the densitometric result which is 12.7±1.5. This disagreement is not related to the difference in affinities and cross-reactivities of recognition IgGs (Fig. 4), since if it were the case, the experimental ratios would result in higher κ:λ values due to overrated kappa and underrated lambda responses.

For HLS, the results are opposite from those of the HKS, and show a higher λ:κ ratio than the densitometric method: 9.7±1.6 *versus* 6.9±0.5. Again, as in the case with HKS, this difference cannot be attributed to the difference in anti-kappa and anti-lambda IgG specificities. In this case the sensor demonstrates a higher sensitivity than the densitometric method suggesting possible limitations in the laboratory approach. The possibility of non-specific binding can be excluded because generally it decreases specificity, and consequently, sensitivity. Another potential explanation, which consists of sensing larger immunoglobulins instead of IgG, should also be excluded because Protein G has no affinity for IgM or IgA.[39] For the direct approach the ratios are lower compared to the reverse approach: 2.6:1 for HKS and 2.6:1 for HLS (Table S5), however in both cases they are still above the normal range suggesting that the direct approach is also applicable.

Reference data for normal serum was not measured but rather estimated based on the 1.4-2.0:1 κ-λ ratio. The experimental κ:λ was 1.8±0.08:1 (Table 3) and 1.7:1 (Table S5) using the reverse and direct approaches respectively, and both fall into the normal region.

Evaluation of the Approaches

Since Protein G has a strong affinity for IgG, when applied in the reverse approach, the Protein G-functionalized surface performs as an immunological filter to capture specifically the analyte of interest (IgG) from the pool of various proteins in serum. As a result, this approach has great potential for reducing non-specific binding since the final recognition step involves purified IgGs in clean buffer and the binding corresponds to immunoglobulin interactions only. Alternatively, in the direct approach, the final sensing step is serum injection and non-specific binding to the anti-human IgG-functionalized surface may occur. Protein G-IgG interaction is limited by the IgG concentration, where the latter must be greater than 50 μg/ml,[33] thus the only requirement for serum dilution is for it to be less than 1:150 for the reverse approach. This is a significant advantage over the direct approach since no prior information on the kappa and lambda immunoglobulin concentration in patient serum is required. For the direct approach, additional information is necessary: a) the initial concentration of IgGκ and IgGλ in patient sera, and b) the sensitivity of the sensor for human:anti-human IgG interaction so that sera can be properly diluted into the linear range to achieve a significant difference in IgGκ and IgGλ responses. Thus, when the reverse approach is applied, detection of B-cell leukemia becomes independent of other preliminary tests and detection techniques. As a summary, from the practical point of view, any patient serum can be diluted with PBS/Gly using a standard dilution factor (<1:150) and used as is. All of the aforementioned points lead to a higher sensitivity of the reverse approach compared to the direct one, which is confirmed by the experimental results. In addition, due to slower binding kinetics of the final analyte in the direct approach (immunoglobulins in patient serum), a longer exposure is preferable (~40 min *vs.* ~20 min in reverse approach) suggesting another advantage of the reverse approach where the total experimental time is reduced.

The only minor disadvantage of the reverse approach is that the extraction of kinetics becomes difficult during the final step due to the RI bulk difference of the sensing buffer and goat anti-human IgG solutions. However, this could be resolved by utilizing lyophilized immunoglobulins mixed with a buffer of controlled RI. The interaction kinetics are primarily of interest for research purposes

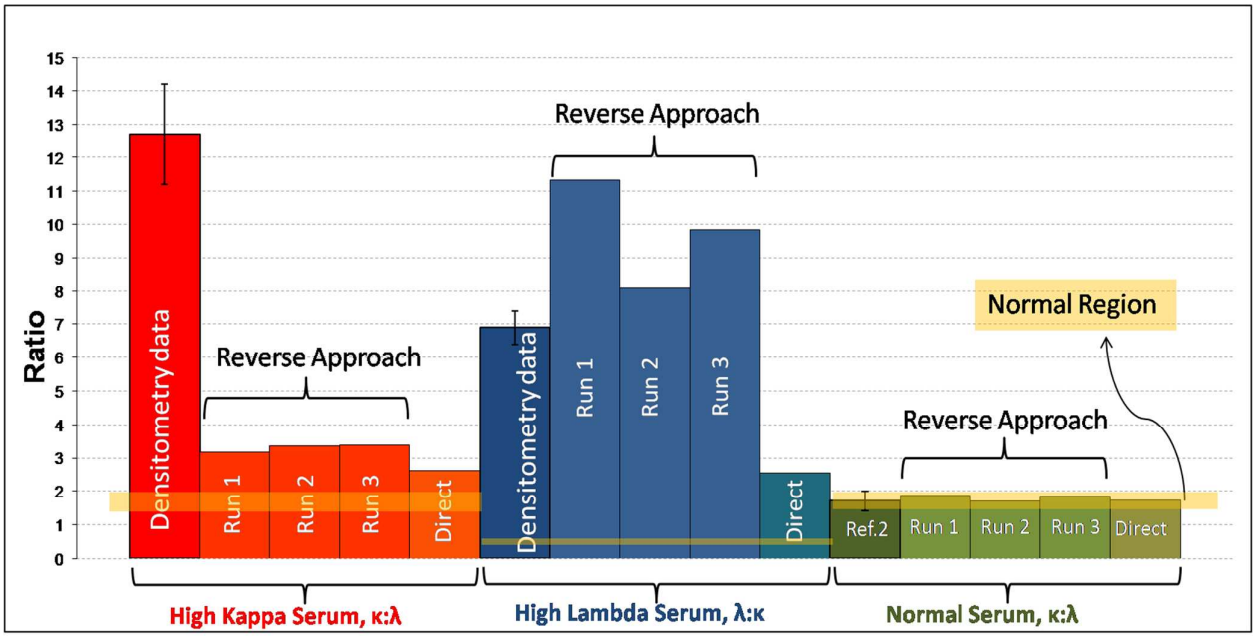

Fig. 6 Kappa-lambda ratios for HKS, HLS and NS obtained using LRSPP sensors. HKS and HLS data are compared to the densitometric data provided by Mount Sinai Hospital laboratory, and NS data is compared to the data in Reference [2].

and do not at present impact diagnosis.

Overall Evaluation

Our LRSPP biosensor demonstrated the capability of differentiating between three patient sera with various κ-λ IgG ratios. The results were compared to densitometric measurements, and found to agree qualitatively but not quantitatively. Nevertheless, the sensor can be used for leukemia biomarker screening. An important advantage of using the sensor compared to common techniques such as densitometry, electrophoresis gel and ELISA is a low consumption of ingredients. Generally, for a half experiment (*e.g.* only IgGκ detection), 10 µg of Protein G, ~ 3 µL of patient serum and 10µg of anti-human IgG are required. The total experimental run duration can also be decreased from 130 to ~100 min by reducing the time for Protein G and human serum immobilization steps, illustrating a further advantage of the sensor relative to lab techniques. Finally, the sensors could be manufactured cheaply and interrogated with an integrated benchtop unit.

Conclusions

LRSPP biosensors were demonstrated for the detection of leukemic biomarkers in patients with B-cell tumors. Three patient sera (two leukemic and one control) were tested for relative concentrations of kappa and lambda light chain immunoglobulins. Two opposite sensing approaches were evaluated and the results were compared to the densitometric data provided by the serum supplier. The reverse approach, where the Au waveguide was functionalized with patient serum first, was found to be more sensitive and more efficient. Several advantages were found for the reverse approach using a Protein G-functionalization surface: a) specific capture of the immunoglobulins out of the pool of serum proteins, b) reduction in non-specific binding during the last sensing step where purified goat anti-human light chain IgGs in clean buffer are injected, and c) no preliminary tests with patient serum are required to determine the κ-λ IgG ratio. Although the LRSPP results differed quantitatively from the laboratory data, a clear differentiation between normal and leukemic sera was achieved. Along with potential miniaturization, the demonstrated LRSPP biosensor can provide a cheap and rapid solution to B-cell tumor screening for clinical diagnostics.

Acknowledgements

The authors gratefully acknowledge NSERC (BiopSys Network) for funding and are grateful to Ritch Dusome and other employees of Cisco (Ottawa) for a philanthropic donation in support of the work. The authors are also grateful to Ewa Lisicka-Skrzek, Sa'ad Hassan and Anthony Olivieri for assistance in carrying out the experiments.

Notes and references

1 American Cancer Society, 2013. Leukemia-Chronic Lymphocytic. American cancer society.
2 J. A. Katzmann, R. J. Clark, R. S. Abraham, S. Bryant, J. F. Lymp, A. R. Bradwell and R. A. Kyle, *Clin.Chem*., 2002. **48**(9), 1437–1444.
3 A. Bradwell, S. Harding, N. Fourrier, C. Mathiot, M. Attal, P. Moreau, J. L. Harousseau, and H. Avet-Loiseau, *Leukemia*, 2013, **27**(1), 202–207
4 J. P. Campbell, M. Cobbold, Y. Wang, M. Goodall, S. L. Bonney, A. Chamba, J. Birtwistle, T. Plant, Z. Afzal, R. Jefferis and M. T. Drayson, *J.Immunol. Methods*, 2013, **39**1(1-2), 1–13.
5 K. M. Charafeddine, M. N. Jabbour, R. H. Kadi and R. T. Daher, *Am.J.Clin.Pathol*., 2012, **137**(6), 890–897.
6 A. R. Bradwell, S. J. Harding, N. J. Fourrier, G. L.F. Wallis, M. T. Drayson, H. D. Carr-Smith and G. P. Mead, *Clin. Chem*., 2009, **55**(9), 1646–1655.
7 M. A. Cooper, *Nat. Rev. Drug Discov.*, 2002, **1**, 515-528.
8 J. Homola, *Chem. Rev.*, 2008, **108**, 4632-493.
9 S. Lofas, *Assay Drug Dev. Technol.*, 2004, **2**, 407-416.
10 P. Berini, *Adv. Opt. Photonics,* 2009, **1**, 484-588.
11 P. Berini, *New J. .Phys.*, 2008, **10**, 1-36.
12 R. Slavík and J. Homola, *Sens. Actuators B,* 2007, **123**, 10-12.
13 Y. H. Joo, S. H. Song and R. Magnusson, *Appl. Phys. Lett.*, 2010, **97**, 201105.
14 A. W. Wark, H. J. Lee and R. M. Corn, *Anal. Chem.*, 2005, **77**, 3904-3907.
15 M. Vala, S. Etheridge, J. Roach and J. Homola, *Sens. Actuators, B,* 2009, **139**, 59-63.
16 V. Chabot, Y. Miron, M. Grandbois and P.G. Charette, *Sens. Actuators, B,* 2012, **174**, 94– 101.
17 A. Boltasseva, T. Nikolajsen, K. Leosson, K. Kjaer, M. S. Larsen, and S. I. Bozhevolnyi, *J. Lightw. Technol.*, 2005, **23**, 413-422.
18 R. Charbonneau, C. Scales, I. Breukelaar, S. Fafard, N. Lahoud, G. Mattiussi and P. Berini, *J. Lightw. Technol.*, 2006, **24**, 477.
19 A. Khan, O. Krupin, E. Lisicka-Skrzek and P. Berini, *Appl. Phys. Lett.*, 2013, **103**, 111108.
20 C. Chiu, E. Lisicka-Skrzek, R. N. Tait and P. Berini, *J. Vac. Sci. Technol. B*, 2010, **28**(4), 729–735.
21 O. Krupin, H. Asiri, C. Wang, R.N. Tait and P. Berini, *Opt. Express*, 2013, **21**, 698-709.
22 O. Krupin, C. Wang and P. Berini, *Biosens. Bioelectron*., 2013, **53**, 117-122.
23 W. R. Wong, O. Krupin, S. D. Sekaran, F. R. Mahamd Adikan and P. Berini, *Anal. Chem.*, 2014, **86**, 1735−1743.
24 P. Beland, O. Krupin and P. Berini, to *Biomed. Opt. Express*., 2015, **6**(8), 2908-2922.
25 W. R. Wong, F. R. M. Adikan and P. Berini, *Appl. Phys. A,* 2014, **117**, 527-535.
26 W.R. Wong, O. Krupin, F.R.M. Adikan and P. Berini, *J. Lightw. Technol.*, 2015, **33**(15), 3234-3242.
27 R. Heideman and P. Lambeck, *Sens. Actuators, B,* 1999, **61**, 100-127.
28 B. Shew, Y. Cheng and Y. Tsai, *Sens. Actuators, A*, 2008, **141**, 299-306.
29 D. Xu, A. Densmore, A. Delâge, P. Waldron, R. McKinnon, S. Janz, J. Lapointe, G. Lopinski, T. Mischki, E. Post, P. Cheben and J. H. Schmid, *Opt. Express,* 2008, **16**, 15137-15148.
30 J. C. Love, L. A. Estroff, J. K. Kriebel, R. G. Nuzzo and G. M. Whitesides, *Chem. Rev.,* 2005, **105**, 1103-1170.
31 J. M. Fowler, M. C. Stuart and D. K. Y. Wong, *Anal. Chem*., 2007, **79**, 350-354.
32 B. N. Johnson and R. Mutharasan, *Langmuir*, 2012, **28**(17),6928–6934.
33 K. Saha, F. Bender and E. Gizeli, *Anal. Chem.*, 2003, **75**, 835-842.
34 M. Maisonneuve, C. Valsecchi, C. Wang, A. G. Brolo and M. Meunier, *Biosens. Bioelectron*., 2015, **63**, 80–85.
35 H. Asiri, (Master's Thesis), Department of Chemistry and Biological Engineering, University of Ottawa, Ottawa, 2012.
36 J. W. Stoop, B. J. M. Zegers, P. C. Sander and R. E. Ballieux, *Clin. Exp. Immunol*., 1969, **4**, 101-112.

37 O. Krupin, C. Wang and P. Berini, "Strategies for leukemic biomarker detection using long-range surface plasmon-polaritons, " 2014, SPIE 9288OW.
38 A. D. Feijter, J. Benjamins and F. A. Veer, *Biopolymers*, 1978, **17**(7), 1759–1772.
39 L. Bjorck and G. Kronvall, *J.Immunol.*, 1984, **133**(2), 969-974.